

Molecular dissociation and two low-temperature high-pressure phases of H<sub>2</sub>SHiroshi Fujihisa,<sup>1</sup> Hiroshi Yamawaki,<sup>1</sup> Mami Sakashita,<sup>1</sup> Atsuko Nakayama,<sup>2</sup> Takahiro Yamada,<sup>1</sup> and Katsutoshi Aoki<sup>3</sup><sup>1</sup>Institute for Materials and Chemical Process, National Institute of Advanced Industrial Science and Technology (AIST),  
1-1-1 Higashi, Tsukuba, Ibaraki 305-8565, Japan<sup>2</sup>Research Center for Advanced Carbon Materials, National Institute of Advanced Industrial Science and Technology (AIST),  
1-1-1 Higashi, Tsukuba, Ibaraki 305-8565, Japan<sup>3</sup>JAERI/SPring-8, 1-1-1, Kouto, Mikazuki-cho, Sayo-gun, Hyogo 679-5148, Japan

(Received 27 January 2004; published 7 June 2004)

We performed powder x-ray experiments on hydrogen sulfide (H<sub>2</sub>S) under high pressure at room and low temperatures. Phase V appearing above 27 GPa at room temperature was confirmed by x ray to be associated with a molecular dissociation. The molecular dissociation was first observed at 150 K at a higher pressure around 43 GPa. Two new low-temperature high-pressure phases III' and IV' were discovered. Spiral chains of sulfur atoms are found in both phases as well as in phase IV.

DOI: 10.1103/PhysRevB.69.214102

PACS number(s): 61.50.Ks, 61.10.Nz, 62.50.+p, 64.70.Kb

## I. INTRODUCTION

Hydrogen sulfide (H<sub>2</sub>S) shows successive phase transitions when cooled. As illustrated at the bottom of Fig. 1, these are phase I (cubic  $Fm\bar{3}m$ ), phase II (cubic  $Pa\bar{3}$ ), and then phase III (orthorhombic  $Pbcm$ ). According to a neutron diffraction experiment,<sup>1</sup> the molecular rotations of phases I and II freeze in phase III. On compression at room temperature, the other successive phase transitions have been observed: phase I,<sup>2</sup> phase I' (cubic  $P2_13$ ), phase IV<sup>2-4</sup> (tetragonal  $I4_1/acd$ )<sup>5</sup> and phase V.<sup>6</sup> The molecular rotations in phases I and I' are thought to stop in phase IV.<sup>2</sup>

Molecular dissociation is one of the interesting phenomena observed in molecular solids under pressure. There have been two opinions of the dissociation pressure of (H<sub>2</sub>S) derived from optical experiments: 46 GPa<sup>7,8</sup> and 27 GPa.<sup>9</sup> A precise interpretation of the Raman and IR spectra of D<sub>2</sub>S<sup>10</sup> revealed that the spectra taken above 27 GPa in the unloading process were identical to those of pure sulfur. The existence of elemental sulfur above 27 GPa has not been confirmed by previous x-ray experiments because all diffraction peaks above this point became too weak to identify its structure.

The hydrogen-bond ordering of H<sub>2</sub>S is also an interesting subject. In a Raman experiment covering pressures up to about 20 GPa,<sup>11</sup> phase boundaries were determined from the spectral changes in the S-H stretching region of 2400–2600 cm<sup>-1</sup>. Obtaining a result indistinguishable from that found from Raman spectra, a neutron diffraction experiment on D<sub>2</sub>S has determined the I'-II boundary to be around 5.3 GPa and 235 K.<sup>12</sup> The atomic positions of rotationally disordered deuterium of phase I' have also been established.<sup>12</sup> No other diffraction study below 200 K and above 6 GPa has been reported. In order to clarify whether the hydrogen bond in phase IV is ordered or not, molecular-dynamics (MD) simulations have been actively pursued.<sup>13-15</sup> If a disordered hydrogen bond remains in phase IV, a new phase with a different bonding state due to ordering should be found at lower temperatures.

Our first purpose was to investigate the molecular dissociation of H<sub>2</sub>S from a structural point of view. To this end,

we performed powder x-ray diffraction experiments up to 48 GPa at room temperature, and found the existence of elemental sulfur above 27 GPa. Our second purpose was to explore a low-temperature high-pressure region from which no diffraction experiments have been reported. In this study, we measured x-ray patterns as low as 30 K and up to 43 GPa, and discovered two new phases.

## II. EXPERIMENTAL

Gaseous H<sub>2</sub>S with a stated purity of 99.999% was solidified in an agate mortar cooled at 77 K by liquid nitrogen. Then the solid H<sub>2</sub>S was ground into a fine powder. The powder was mounted on a diamond anvil high-pressure cell

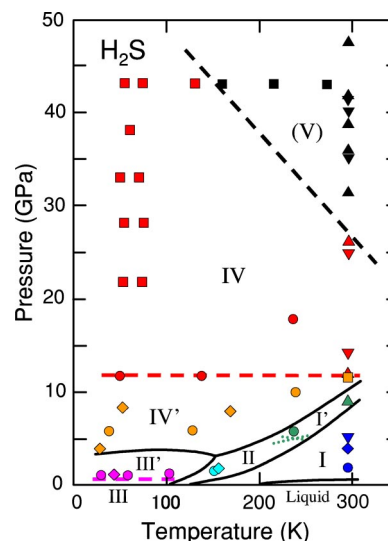


FIG. 1. (Color online) The pressure-temperature phase diagram of H<sub>2</sub>S. The solid curves are phase boundaries determined by a Raman experiment.<sup>11</sup> The dotted lines between I' and II are determined by a neutron experiment.<sup>12</sup> The triangles (run 1), the inverse triangles (run 2), the circles (run 3), the diamonds (run 4), and the squares (run 5) show the measured points from five independent samples. Three dashed lines are determined in this report.

(DAC) cooled down to 77 K, pressurized to a few GPa, and warmed up to room temperature while holding the pressure constant. These operations were carried out in a gaseous nitrogen atmosphere to avoid an H<sub>2</sub>O frost.

Five independent experimental runs were carried out at room and low temperatures. In runs 1 and 2, for experiments at room temperature, a sample chamber of 100  $\mu\text{m}$  in diameter and 40  $\mu\text{m}$  in thickness was made by drilling a hole into a rhenium foil. In runs 3 and 4, for experiments up to 20 GPa at low temperature, a sample chamber of 130  $\mu\text{m}$  in diameter and 80  $\mu\text{m}$  in thickness was prepared. A sample chamber of 70  $\mu\text{m}$  in diameter and 40  $\mu\text{m}$  in thickness was set up for run 5 which was designed for an experiment with pressures up to 50 GPa at low temperature. In runs 3, 4, and 5, respectively, a rhenium, an SUS301 (an austenite stainless steel), and a PK (a spring steel, Fe 98%) gasket were used. The DAC pressure was controlled by introducing helium gas through a cryostat chamber into a membrane chamber attached to the DAC itself. The temperatures were monitored by two Si diode sensors and two thermocouples placed on the DAC holders.

Angle-dispersive powder x-ray diffraction experiments were performed on the BL-18C beam line at the Photon Factory of the High Energy Accelerator Research Organization (KEK). The x-ray beams were monochromatized to a wavelength of 0.6198  $\text{\AA}$  (20.00 keV) and the diffracted x rays were recorded on an imaging-plate (IP) detector supplied by Fuji Photo Film Co., Ltd. Typical exposure times were 1 h for the room temperature experiments and 5 min for the low-temperature experiments. The samples thus prepared gave smooth Debye-Scherrer rings and no contamination peaks of H<sub>2</sub>O which led to reliable structure analyses.

### III. ROOM-TEMPERATURE RESULTS

In agreement with previous reports, the successive phase transitions at room temperature were observed in runs 1 and 2. Figure 2(a) displays the powder diffraction pattern of phase V at 42 GPa. The peaks, first appearing at about 27 GPa, grew continuously until a pressure of 48 GPa was reached, though a characteristic high background level was evident. The vertical bars in Fig. 2(a) represent the positions and the intensities measured for the high-pressure sulfur phase II at 42 GPa by Akahama.<sup>16</sup> They corresponded well to the peaks of phase V, with an exception of one peak at 13.5 degrees ( $d=2.64$   $\text{\AA}$ ). As suggested by Sakashita,<sup>10</sup> this peak possibly comes from an intermediate component that still has an S-H bond. Phase I of elemental sulfur ( $\alpha$ -S<sub>8</sub>) undergoes amorphization from 18–27 GPa, and on further compression, a crystalline phase II appears.<sup>17,18</sup> These findings suggest that the origin of the high background observable in Fig. 2(a) can be attributed to the existence of the amorphous phase of sulfur.

The presence of solid sulfur was confirmed by an unloading experiment. Here, the diffraction patterns showed no change until 5 GPa. With a further decrease in pressure to about 1 GPa, a part of the sample bubbled and leaked from the sample chamber, but most of the sample remained solid even at ambient conditions. To examine its structure, we

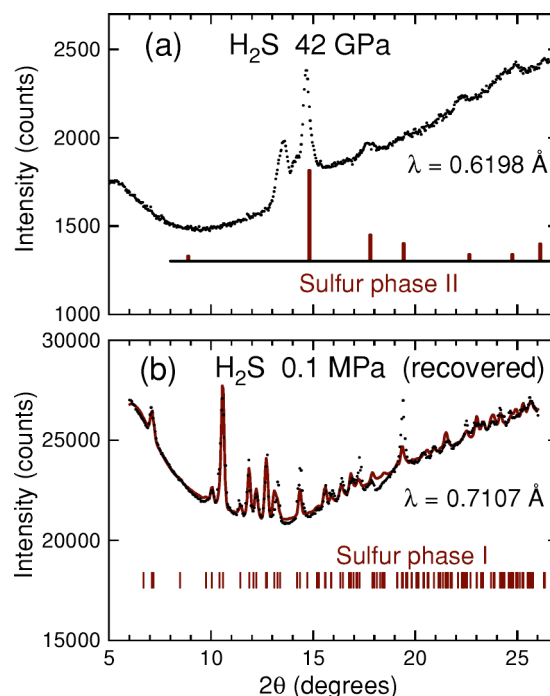


FIG. 2. (Color online) (a) The powder pattern of H<sub>2</sub>S obtained at 42 GPa. (b) The powder pattern of recovered sample after unloading from 48 GPa to ambient. The negative slopes of the backgrounds below 9 degrees are due to air scattering of the direct beams.

measured the diffraction pattern for the recovered sample using a conventional 18 kW x-ray generator with a Mo rotating anode (0.7107  $\text{\AA}$ ), an 80  $\mu\text{m}$  pin-hole collimator, and the IP for 50 h of exposure. The dots and the profile in Fig. 2(b) represent the powder diffraction pattern and the Rietveld fit produced with the most likely candidate structure of sulfur phase I. The solid was thus found to contain a form of sulfur phase I, consisting of S<sub>8</sub> rings. The pattern's background level, arising from the remaining amorphous component, was still high.

The x-ray data revealed that the molecular dissociation of the H<sub>2</sub>S started at 27 GPa at room temperature, a result in good agreement with the results of the previous optical measurement.<sup>9,10</sup> After the dissociation, the sample behaved like elemental sulfur. This may explain why the metallization pressure of 96 GPa reported for H<sub>2</sub>S<sup>8</sup> is very close to that of 95 GPa for sulfur.<sup>18</sup> In further agreement with the results of optical experiments, the x-ray results indicate that phases V and VI are not pure phases of H<sub>2</sub>S.<sup>10</sup> Since the results did not depend on the chemical identity of the gasket, the dissociation is not likely to be initiated by a chemical reaction with gasket material.

### IV. LOW-TEMPERATURE RESULTS

The patterns obtained in runs 3 and 4 at 1 GPa below 100 K were different from those of phase III (*Pbcm* Ref. 1). We name this phase III'. A Rietveld analysis, shown in

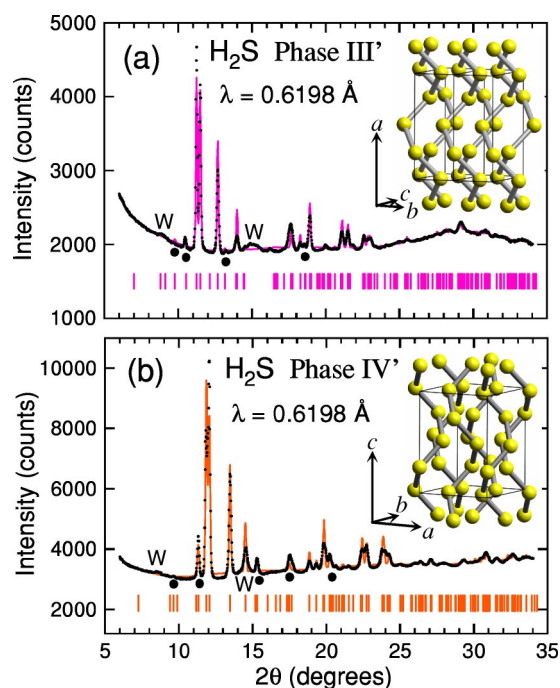


FIG. 3. (Color online) Rietveld fits and their derived structures of (a)  $\text{H}_2\text{S}$  phase III' at 1.1 GPa and 38 K, and (b)  $\text{H}_2\text{S}$  phase IV' at 3.8 GPa and 27 K. Broad peaks labeled W represent diffraction from the plastic film of the cryostat window. The solid circles beneath the patterns show the differences between phases III' and IV'.

Fig. 3(a), revealed that its structure belongs to an orthorhombic space group  $Pcca$  made up of eight molecules in the unit cell. The lattice parameters at 1.1 GPa and 38 K were  $a = 10.189 \pm 0.001 \text{ \AA}$ ,  $b = 4.040 \pm 0.001 \text{ \AA}$ ,  $c = 7.809 \pm 0.001 \text{ \AA}$ . The sulfur atoms were located on two different sites:  $4c$  ( $0, y = 0.469 \pm 0.004, 1/4$ ) and  $4d$  ( $1/4, 0, z = 0.017 \pm 0.002$ ). The inset of Fig. 3(a) displays the structure without hydrogen. The first nearest neighbor S-S distance, depicted with sticks, was  $3.67 \pm 0.03 \text{ \AA}$ . One can see spiral chains along the  $a$ -axis, just as was found in phase IV.<sup>5</sup> At 1.1 GPa and room temperature, the first nearest neighbor S-S distance of phase I is  $3.9 \text{ \AA}$ ; the molecules are hydrogen bonded. Since the value of the S-S distance in phase III' of  $3.67 \pm 0.03 \text{ \AA}$  is significantly shorter than the  $3.9 \text{ \AA}$  seen in phase I, the molecules in phase III' are not hydrogen bonded.

A new intermediate phase was observed in the region of 4–10 GPa and 30–250 K; this region is in contact with the boundaries of phases III', II and I', and has been considered to be stable for a tetragonal phase IV. We name this phase IV'. By a Rietveld analysis, as shown in Fig. 3(b), its space group was determined to be an orthorhombic  $Ibca$  including 16 molecules. The lattice parameters at 3.8 GPa and 27 K were  $a = 7.574 \pm 0.001 \text{ \AA}$ ,  $b = 7.389 \pm 0.001 \text{ \AA}$ ,  $c = 9.829 \pm 0.002 \text{ \AA}$ . The sulfur atoms were located on two different sites:  $8c$  ( $x = 0.010 \pm 0.004, 0, 1/4$ ) and  $8d$  ( $1/4, y = 0.206 \pm 0.003, 0$ ). The axial ratio  $a/b$  was 1.025 at 3.8 GPa, decreasing with pressure to almost 1.0 at 12.0 GPa. It became hard to judge whether the strongest peak of the 12 GPa data at 54 K, 138 K, and room temperature was a doublet or

a singlet. Hence, in Fig. 1 we located a temperature insensitive horizontal line at 12 GPa, shown with the dashed line. The inset of Fig. 3(b) displays the structure without hydrogen atoms. The first nearest neighbor S-S distance was  $3.41 \text{ \AA}$  at 3.8 GPa. As in phases IV and III', we can see spiral chains. A low-temperature high-pressure phase, which has been observed by Raman measurement at 25 K in a pressure span of 3.3–8.0 GPa,<sup>19</sup> is now identified as this phase IV'. The report has already mentioned that the Raman spectra at 25 K drastically changed from 0 to 3 GPa. This very likely corresponds to successive phase transitions of III-III'-IV'.

In run 5, the molecular dissociation was investigated along an isobar line at 43 GPa warming from 49 to 270 K. It was first observed at 150 K, a temperature almost one half of that (298 K) for the onset of dissociation at 27 GPa. The boundary showed a negative slope of  $-0.11 \text{ GPa/K}$ , as illustrated by the dashed line at the top right of Fig. 1. We additionally measured Raman spectra of this dissociated sample at room temperature in its unloading process from 48 to 4 GPa to examine existence of hydrogen molecules. The S-S peaks were clearly observed around  $500 \text{ cm}^{-1}$  as same as the  $\text{D}_2\text{S}$  study.<sup>10</sup> In spite of an hour accumulation with a 1 mW Ar ion laser at the sample position, there were no trace of the H-H vibration around  $4200 \text{ cm}^{-1}$ . The separated hydrogen atoms may creep into the sulfur lattice, the gasket, or the diamond anvils.

## V. DISCUSSION

Phases III', IV' and V have similar intrachain and inter-chain bonds and can exist below 100 K, at which point all molecular rotations must stop. The existence of phases IV' and IV from 25 K to room temperature means that the same bonding state has been kept. Therefore, the hydrogen bonds in these phases would be fully ordered, even at room temperature. The contradiction in the MD,<sup>13,15</sup> as to whether the hydrogen bond in phase IV is ordered or disordered, has now been clarified experimentally.

Figure 4 displays the pressure dependence of the interatomic distances of the sulfur atoms for phases I, II', III', IV, and IV'. Since the variation of distances with temperature was thought to be much smaller than that with pressure, no data for variation of temperature was included in the plot. Each first nearest-neighbor distance of phases III', IV', and IV corresponds to the intrachain distance (S-S distance), and, hence, can be used for discussion of the nature of the bond between the sulfur atoms. The S-S distance of phase III' ( $3.67 \text{ \AA}$  at 1.1 GPa) is almost same as the shortest S-S contact distance of phase III [ $3.672 \text{ \AA}$  at 0 GPa (Ref. 1)]. They are close to twice the sulfur van der Waals radius ( $3.60 \text{ \AA}$ ) shown with  $vdW$  in Fig. 4. On the other hand, the long distances in phase III [ $4.280$  and  $4.382 \text{ \AA}$  (Ref. 1)], which contain no hydrogen atoms, are compressed efficiently below  $4.04 \text{ \AA}$  in phase III' by pressure. In phase IV' where the S-S from  $3.41$  to  $3.12 \text{ \AA}$ , the electron clouds of the sulfur atoms must somehow overlap each other. In our previous data concerning phase IV at room temperature,<sup>5</sup> the S-S distance shrank down to  $2.96 \text{ \AA}$  at the highest pressure reached,

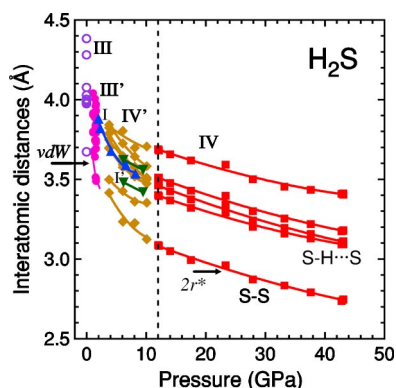


FIG. 4. (Color online) Interatomic sulfur-sulfur distances of  $\text{H}_2\text{S}$  under pressure. The data drawn with the triangles, the inverse triangles, the circles, the diamonds, and the squares correspond to the phases I, I', III', IV', and IV, respectively. Our previous data for phases I, I', and IV at room temperature (Ref. 5) are included in this plot. The open circles at 0 GPa show the phase III data at 1.5 K (Ref. 1). The horizontal arrows represent twice the sulfur van der Waals radius ( $vdW$ ) and twice the sulfur constant energy radius ( $2r^*$ ). The vertical dashed line represents the IV'-IV boundary at 12.0 GPa.

23.3 GPa. the sulfur constant energy radius of 2.92 Å (Ref. 20) shown with  $2r^*$  in Fig. 4, which is a criterion for the existence of overlap of the molecular orbitals or of covalent bond formation.<sup>10,21</sup> The present low-temperature experiment extended significantly the pressure span for structural measurement as a result of the suppression of the dissociation reaction, and the S-S distances of phase IV were measured up to 43 GPa. The S-S distance decreases to 2.74 Å at a pressure of 43 GPa, below beyond the critical value of 2.92 Å. At this pressure, intrachain covalency should strengthen. After the dissociation, this S-S interaction may become fully covalent bonds in sulfur phase II and amorphous sulfur.

The dissociation process has been precisely investigated by a recent UV-visible-IR absorption measurement, and was shown to be initiated photochemically or thermally by laser irradiation above 24 GPa.<sup>21</sup> The slope of  $-0.11$  GPa/K indicates that a temperature elevation of just 30 K above room temperature decreases the dissociation pressure to 24 GPa. Therefore we conclude that the dissociation is induced thermally. It should be noted that all transitions of  $\text{H}_2\text{S}$  including the molecular dissociation did not depend on x-ray wavelength, intensity, nor exposure time. Therefore the dissociation would not be affected by the x-ray probe itself.

Endo *et al.* have proposed a monoclinic  $Pc$  structure for phase IV.<sup>22</sup> This structure shows complicated distortions in atomic arrangement and interatomic distances due to its very low symmetry. The monoclinic cell with the same length of  $a$  and  $c$  axes might be converted to an orthogonal system. The 11.4 GPa diffraction pattern they used for structural analysis involved the strongest peak with the doublet feature. Our pattern at 11.9 GPa at room temperature also showed the doublet feature for the strongest peak, and the overall profile was essentially in agreement with that of the 11.4 GPa data. By a Rietveld analysis, the pattern was satisfactorily reproduced with the phase IV' model of the orthorhombic  $Ibca$  structure. The relationship between the  $Pc$  cell ( $\mathbf{a}_m, \mathbf{b}_m, \mathbf{c}_m$ ) and the  $Ibca$  cell ( $\mathbf{a}_0, \mathbf{b}_0, \mathbf{c}_0$ ) was written as:  $\mathbf{a}_0 = \mathbf{a}_m + \mathbf{c}_m$ ,  $\mathbf{c}_0 = \mathbf{c}_m - \mathbf{a}_m$ ,  $\mathbf{b}_0 = 2\mathbf{b}_m$ . Thus the previous pattern was taken at 11.4 GPa in a stable region of phase IV' and could be explained as consistent with the  $Ibca$  structure which is preferable to the  $Pc$  structure.

## ACKNOWLEDGMENTS

The present work was carried out as a part of the CREST (Core Research for Evolutional Science and Technology) project of the Japan Science and Technology Corporation and with the approval of the Photon Factory Program Advisory Committee (Proposal Nos. 98G272 and 00G202).

<sup>1</sup>J. K. Cockcroft and A. N. Fitch, *Z. Kristallogr.* **193**, 1 (1990).

<sup>2</sup>H. Shimizu, Y. Nakamichi, and S. Sasaki, *J. Chem. Phys.* **95**, 2036 (1991).

<sup>3</sup>S. Endo, N. Ichimiya, K. Koto, S. Sasaki, and H. Shimizu, *Phys. Rev. B* **50**, 5865 (1994).

<sup>4</sup>H. Shimizu, H. Murashima, and S. Sasaki, *J. Chem. Phys.* **97**, 7137 (1992).

<sup>5</sup>H. Fujihisa, H. Yamawaki, M. Sakashita, K. Aoki, S. Sasaki, and H. Shimizu, *Phys. Rev. B* **57**, 2651 (1998).

<sup>6</sup>S. Endo, A. Honda, S. Sasaki, H. Shimizu, O. Shimomura, and T. Kikegawa, *Phys. Rev. B* **54**, R717 (1996).

<sup>7</sup>H. Shimizu, T. Ushida, S. Sasaki, M. Sakashita, H. Yamawaki, and K. Aoki, *Phys. Rev. B* **55**, 5538 (1997).

<sup>8</sup>M. Sakashita, H. Yamawaki, H. Fujihisa, K. Aoki, S. Sasaki, and H. Shimizu, *Phys. Rev. Lett.* **79**, 1082 (1997).

<sup>9</sup>M. Yamagishi, H. Furuta, S. Endo, and M. Kobayashi, in *Science*

*and Technology of High Pressure*, edited by M. H. Manghnani, W. J. Nellis, and M. F. Nicol (Universities Press, Hyderabad, 2000), p. 391.

<sup>10</sup>M. Sakashita, H. Fujihisa, H. Yamawaki, and K. Aoki, *J. Phys. Chem. A* **104**, 8838 (2000).

<sup>11</sup>H. Shimizu, H. Yamaguchi, S. Sasaki, A. Honda, S. Endo, and M. Kobayashi, *Phys. Rev. B* **51**, 9391 (1995).

<sup>12</sup>J. S. Loveday, R. J. Nelmes, S. Klotz, J. M. Besson, and G. Hamel, *Phys. Rev. Lett.* **85**, 1024 (2000).

<sup>13</sup>R. Rousseau, M. Boero, M. Bernasconi, M. Parrinello, and K. Terakura, *Phys. Rev. Lett.* **83**, 2218 (1999).

<sup>14</sup>T. Ikeda, *Phys. Rev. B* **64**, 104103 (2001).

<sup>15</sup>R. Rousseau, M. Boero, M. Bernasconi, M. Parrinello, and K. Terakura, *Phys. Rev. Lett.* **85**, 1254 (2000).

<sup>16</sup>Y. Akahama (private communication).

<sup>17</sup>Y. Akahama, M. Kobayashi, and H. Kawamura, *Phys. Rev. B* **48**,

- 6862 (1993).
- <sup>18</sup>H. Luo, S. Desgreniers, Y. K. Vohra, and A. L. Ruoff, *Phys. Rev. Lett.* **67**, 2998 (1991).
- <sup>19</sup>A. Anderson, S. Demoor, and R. C. Hanson, *Chem. Phys. Lett.* **140**, 471 (1987).
- <sup>20</sup>M. L. Huggins, *J. Am. Chem. Soc.* **75**, 4126 (1953).
- <sup>21</sup>T. Kume, Y. Fukaya, S. Sasaki, and H. Shimizu, *Rev. Sci. Instrum.* **73-6**, 2355 (2002).
- <sup>22</sup>S. Endo, A. Honda, K. Koto, O. Shimomura, T. Kikegawa, and N. Hamaya, *Phys. Rev. B* **57**, 5699 (1998).